

# A theory framework for scrape-off layer turbulence in limited tokamaks

F.D. Halpern\*, P. Ricci, S. Jolliet<sup>†</sup>, J. Loizu<sup>‡</sup>, A. Masetto, F. Riva, C. Wersal

*École Polytechnique Fédérale de Lausanne, Centre de Recherches en Physique des Plasmas,  
CH-1015 Lausanne, Switzerland*

In the present work we address the physical mechanisms determining the SOL width of a simple inner-wall limited (IWL) configuration. This seemingly simple configuration has important implications for ITER start-up plasmas, and has triggered an important ITPA-sponsored effort to understand the decay length of the heat-flux width. In the past few years, we developed a theoretical understanding of the physical processes regulating the IWL-SOL width, based on computational and analytical investigations.

Our theory framework involves, in particular, SOL profile formation as a power balance between plasma injection from the closed-field-line region, perpendicular fluxes, and parallel losses at the limiter. Experimental observations of the SOL show strong fluctuations with  $n/\langle n \rangle_t \sim 1$ , poloidal mode width  $k_y^{-1} \approx 10\rho_s$ , a large radial mode extension, and intermittent transport events driven by coherent plasma filaments (blobs). For this reason, we have carried out thorough numerical studies to understand and characterize the linear and non-linear turbulent SOL dynamics using a global, flux-driven approach.

In order to address SOL turbulent phenomena we have developed the Global Braginskii Solver (GBS), a numerical implementation of the electromagnetic, drift-reduced Braginskii fluid model [1]. These equations are appropriate for low-frequency, field-aligned turbulence in the Braginskii (collisional) regime. Recently, the code has been upgraded to include finite ion temperature effects. The equations implemented in the code are as follows:

$$\frac{\partial n}{\partial t} = -\rho_\star^{-1}[\phi, n] + \frac{2}{B}[C(p_e) - nC(\phi)] - \nabla_\parallel \cdot (nv_{\parallel e}) + S_n \quad (1)$$

$$\frac{\partial \nabla_\perp^2 \phi}{\partial t} = -\rho_\star^{-1}[\phi, \nabla_\perp^2 \phi] - v_{\parallel i} \nabla_\parallel \nabla_\perp^2 \phi + \frac{B^2}{n} \nabla_\parallel j_\parallel + \frac{2B}{n} C(p) \quad (2)$$

$$\frac{\partial \chi}{\partial t} = -\rho_\star^{-1}[\phi, v_{\parallel e}] - v_{\parallel e} \nabla_\parallel v_{\parallel e} + \frac{m_i}{m_e} \left( v \frac{j_\parallel}{n} + \nabla_\parallel \phi - \frac{1}{n} \nabla_\parallel p_e - 0.71 \nabla_\parallel T_e \right) \quad (3)$$

$$\frac{\partial v_{\parallel i}}{\partial t} = -\rho_\star^{-1}[\phi, v_{\parallel i}] - v_{\parallel i} \nabla_\parallel v_{\parallel i} - \frac{1}{n} \nabla_\parallel p \quad (4)$$

$$\begin{aligned} \frac{\partial T_e}{\partial t} = & -\rho_\star^{-1}[\phi, T_e] - v_{\parallel e} \nabla_\parallel T_e + \frac{4}{3} \frac{T_e}{B} \left[ \frac{1}{n} C(p_e) + \frac{5}{2} C(T_e) - C(\phi) \right] \\ & + \frac{2}{3} T_e [0.71 \nabla_\parallel j_\parallel - \nabla_\parallel v_{\parallel e}] + S_{T_e} \end{aligned} \quad (5)$$

\*Corresponding author: federico.halpern@epfl.ch

<sup>†</sup>Present address: Vaudoise Assurances, Avenue de Cour 41, 1007 Lausanne, Suisse

<sup>‡</sup>Present address: Max Planck Princeton Center for Plasma Physics, Princeton, NJ 08544, USA

$$\begin{aligned} \frac{\partial T_i}{\partial t} = & -\rho_\star^{-1}[\phi, T_i] - v_{\parallel i} \nabla_{\parallel} T_i + \frac{4 T_i}{3 B} \left[ C(T_e) + \frac{T_e}{n} C(n) - C(\phi) \right] \\ & + \frac{2}{3} T_i (v_{\parallel i} - v_{\parallel e}) \frac{\nabla_{\parallel} n}{n} - \frac{2}{3} T_i \nabla_{\parallel} v_{\parallel e} - \frac{10 T_i}{3 B} C(T_i) \end{aligned} \quad (6)$$

The normalizations used are defined in Ref. [2]. GBS is capable of carrying out massively parallel simulations of SOL plasma dynamics, involving plasma profile formation in the SOL as a power balance between plasma flux from the core, the turbulent radial transport, and the losses at the plasma sheath where the magnetic field lines intersect with the vessel. Recently, GBS has been subject to a rigorous verification procedure using the manufactured solutions method, which unequivocally demonstrated the correct numerical implementation of the model equations [3].

An extensive simulation scan was carried out, revealing the instabilities driving turbulent transport [4], the mechanisms that lead to turbulent saturation [5], the role of  $T_i$  fluctuations, the equilibrium electric field [6], toroidal rotation [7], aspect ratio effects [8], and the role of electromagnetic flutter [9, 2], leading to an extensive framework describing the turbulent properties of the system. Moreover, we have addressed for the first time the plasma size scaling of the SOL width by means of a dedicated simulation scan, which demonstrated a widening of the SOL as  $\rho_\star$  decreases [2]. Within the scan, we varied the dimensionless Spitzer resistivity  $\nu = 0.01-1$ ,  $\beta$  was varied from electrostatic to ideal unstable regime,  $q = 3, 4, 6$ , and the plasma size  $\rho_\star$  reached the size of a medium size tokamak such as TCV.

We now concentrate on the phenomena affecting the SOL width. The dynamics observed in the simulations can be described as follows. First, it was inferred that turbulent saturation mechanisms such as Kelvin-Helmholtz secondary instability are typically weak in the SOL. Therefore, modes saturate when they are able to remove that driving plasma gradients [5]. The *gradient removal* hypothesis, gives an estimate of the radial width of the saturated mode,  $\sigma_x/L_p \sim p_1/\langle p \rangle_t$ . Power balance between  $\mathbf{E} \times \mathbf{B}$  radial turbulent fluxes and parallel losses at the sheath  $\sim p_0/q$  lead to an estimate of the SOL width

$$\frac{L_p}{q} = \left( \frac{\gamma}{k_y} \right)_{\max}, \quad (7)$$

where we consider a single poloidal mode which maximizes the flux. The radial width of the mode is assumed to be meso-scale with  $\sigma_x = \sqrt{L_p/k_y}$ . Equation 7 gives an estimate of the SOL width, which was verified against GBS non-linear simulations yielding excellent agreement (Fig. 1, left). A quasi-linear study was then carried out, using reduced analytical models, to determine which instability is responsible for the turbulent transport observed in the simulations [4]. These results were again compared with GBS non-linear simulations, confirming

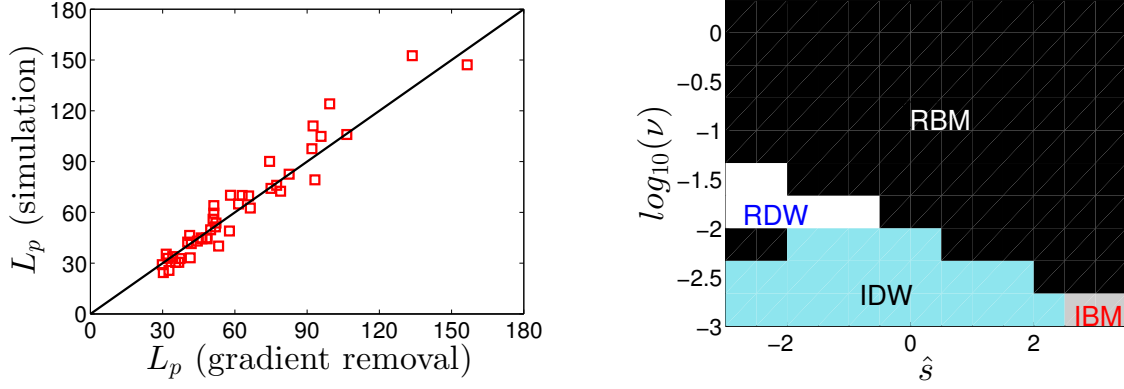


Figure 1: *Left: Comparison between gradient removal mechanism and GBS non-linear simulation results [2]. Right: Non-linear turbulent regimes as a function of dimensionless plasma parameters [4]. The instabilities driving transport in each regime are resistive or inertial drift waves or ballooning modes, abbreviated as RDW/IDW/RBM/IBM.*

the parameter regimes where the resistive and inertial branches of drift wave and ballooning instabilities are relevant (Fig. 1, right).

The results presented in Fig. 1 can easily be related to typical experimental parameters. Taking TCV as an example ( $R = 0.88\text{m}$ ,  $B = 1.4\text{T}$ ,  $T_{e,SOL} \approx 15\text{eV}$ ,  $n_{e,SOL} \approx 3 \times 10^{18}\text{m}^3$ ) we obtain  $\rho_*^{-1} = 2000$ ,  $\nu = 0.01$ ,  $\beta \approx 10^{-5}$ , while  $q = 3-6$  and  $\hat{s} \approx 2$ . GBS simulations with parameters equivalent to the TCV SOL were carried out, showing that resistive ballooning modes (RBMs) were responsible for the turbulent transport. Thus, a simple analytical estimate for the SOL width can be computed using Eq. 7 together with the solution of a linear dispersion relation for RBMs. In fact, by maximizing  $\gamma/k_y$  for RBMs it can be shown analytically that modes driving transport have  $k_y = k_b \propto \nu^{-1/2} q^{-1} \rho_*^{1/2} L_p^{1/2}$  and  $\gamma \propto \gamma_b = \sqrt{2\rho_*^{-1} L_p^{-1}}$ . Inserting this result into Eq. 7 yields a dimensionless scaling for the SOL width measured in  $\rho_s$ :

$$L_p = 2^{3/7} q^{8/7} \rho_*^{-3/7} \nu^{2/7}, \quad (8)$$

which translated into MKSA units yields

$$L_p = 7.22 \times 10^{-8} q^{8/7} R^{5/7} B_\phi^{-4/7} T_{e,SOL}^{2/7} n_{e,SOL}^{-2/7} \left(1 + \frac{T_{i,SOL}}{T_{E,SOL}}\right) [m]. \quad (9)$$

A comparison between these two scalings, GBS simulations, and experimental data is plotted in Fig. 2, showing good agreement.

Since the match between simulation results and the dimensionless scaling is not perfect, it is worth investigating the cause of this disagreement. Brute force regression of the simulation data yields a slightly different scaling:

$$L_p = q^{0.98} \rho_*^{-0.46} \nu^{0.17}. \quad (10)$$

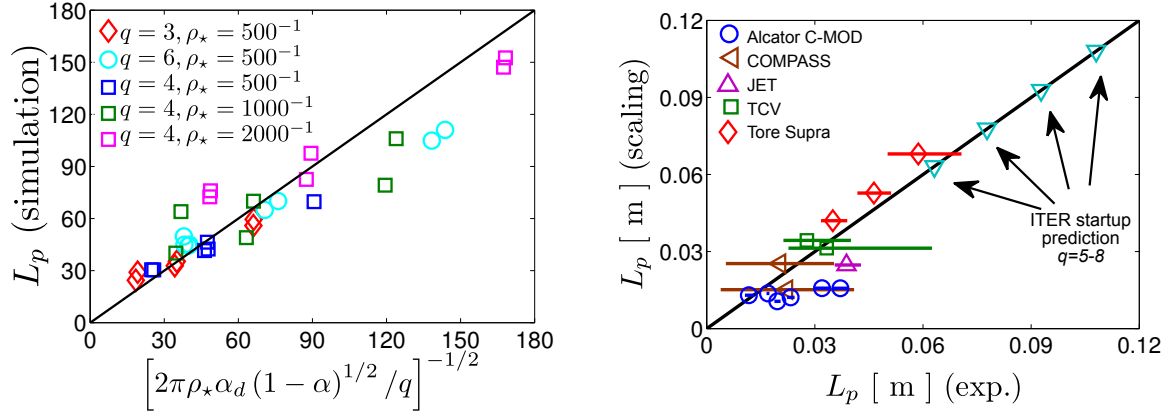


Figure 2: *Left: Comparison between dimensionless scaling (Eq. 8) and GBS non-linear simulation results [2]. Right: Comparison between engineering parameter scaling (Eq. 9) and experimental data points [10].*

It was found that the disagreement between Eq. 8 and Eq. 9 is due to a combination of effects. In particular, (a) GBS simulations were carried out with an artificially large electron mass, which enhanced the inertial ballooning component in the simulations and (b) Eq. 8 was derived under the assumption of full non-adiabaticity, a condition that is not fulfilled in GBS due to the coupling of density and potential fluctuations.

In conclusion, the non-linear dynamics revealed by the simulations are in excellent agreement with reduced models. This advance has allowed the development of a simple SOL width scaling, which shows good agreement when compared against experimental data from several tokamaks [10].

## Acknowledgements

We would like to thank G. Arnoux, I. Furno, J. Gunn, J. Horacek, M. Kočan, B. Labit, B. LaBombard, and C. Silva for providing the experimental measurements shown in Fig. 2.

## References

- [1] P. Ricci, *et al.*, Plasma Physics and Controlled Fusion **54**, 124047 (2012).
- [2] F. Halpern, *et al.*, Nuclear Fusion **54**, 043003 (2014).
- [3] F. Riva, *et al.*, Physics of Plasmas **21**, 062301 (2014).
- [4] A. Masetto, *et al.*, Physics of Plasmas **20**, 092308 (2013).
- [5] P. Ricci and B. N. Rogers, Physics of Plasmas **20**, 010702 (2013).
- [6] J. Loizu, *et al.*, Plasma Physics and Controlled Fusion **55**, 124019 (2013).
- [7] J. Loizu, *et al.*, Physics of Plasmas (in press), **21** (2014).
- [8] S. Jolliet, *et al.*, Physics of Plasmas **21**, 022303 (2014).
- [9] F. D. Halpern, *et al.*, Physics of Plasmas **20**, 052306 (2013).
- [10] F. Halpern, *et al.*, Nuclear Fusion **53**, 122001 (2013).